

ARTICLE

Received 11 Apr 2014 | Accepted 23 Jul 2014 | Published 12 Sep 2014

DOI: 10.1038/ncomms5784

OPEN

Comparative genome sequencing reveals genomic signature of extreme desiccation tolerance in the anhydrobiotic midge

Oleg Gusev^{1,2,3,*}, Yoshitaka Suetsugu^{1,*}, Richard Cornette^{1,*}, Takeshi Kawashima⁴, Maria D. Logacheva^{5,6,7}, Alexey S. Kondrashov^{5,8}, Aleksey A. Penin^{5,7,9}, Rie Hatanaka¹, Shingo Kikuta¹, Sachiko Shimura¹, Hiroyuki Kanamori¹, Yuichi Katayose¹, Takashi Matsumoto¹, Elena Shagimardanova², Dmitry Alexeev¹⁰, Vadim Govorun¹⁰, Jennifer Wisecaver¹¹, Alexander Mikheyev⁴, Ryo Koyanagi⁴, Manabu Fujie⁴, Tomoaki Nishiyama¹², Shuji Shigenobu^{13,14}, Tomoko F. Shibata¹³, Veronika Golygina¹⁵, Mitsuyasu Hasebe^{13,14}, Takashi Okuda¹, Nori Satoh⁴ & Takahiro Kikawada¹

Anhydrobiosis represents an extreme example of tolerance adaptation to water loss, where an organism can survive in an ametabolic state until water returns. Here we report the first comparative analysis examining the genomic background of extreme desiccation tolerance, which is exclusively found in larvae of the only anhydrobiotic insect, *Polypedilum vanderplanki*. We compare the genomes of *P. vanderplanki* and a congeneric desiccation-sensitive midge *P. nubifer*. We determine that the genome of the anhydrobiotic species specifically contains clusters of multi-copy genes with products that act as molecular shields. In addition, the genome possesses several groups of genes with high similarity to known protective proteins. However, these genes are located in distinct paralogous clusters in the genome apart from the classical orthologues of the corresponding genes shared by both chironomids and other insects. The transcripts of these clustered paralogues contribute to a large majority of the mRNA pool in the desiccating larvae and most likely define successful anhydrobiosis. Comparison of expression patterns of orthologues between two chironomid species provides evidence for the existence of desiccation-specific gene expression systems in *P. vanderplanki*.

¹ National Institute of Agrobiological Sciences (NIAS), Tsukuba 305-8602, Japan. ² Institute of Fundamental Biology and Medicine, Kazan Federal University, Kazan 420008, Russia. ³ ISS Science Project Office, Institute of Space and Astronautical Science, Japan Aerospace Exploration Agency (JAXA), Tsukuba 305-8505, Japan. ⁴ Okinawa Institute of Science and Technology Graduate University (OIST), Onna, Okinawa 904-0495, Japan. ⁵ Department of Bioengineering and Bioinformatics, Lomonosov Moscow State University, Moscow 119991, Russia. ⁶ A. N. Belozersky Research Institute of Physico-Chemical Biology, Lomonosov Moscow State University, Moscow 119991, Russia. ⁷ Institute for Information Transmission Problems of the Russian Academy of Sciences, Moscow 127994, Russia. ⁸ Life Sciences Institute and Department of Ecology and Evolutionary Biology, University of Michigan, Ann Arbor, Michigan 48109, USA. ⁹ Department of Genetics, Faculty of Biology, Lomonosov Moscow State University, Moscow 119991, Russia. ¹⁰ Scientific Research Institute of Physico-Chemical Medicine, Federal Bio-Medical Agency of Russia, Moscow 119828, Russia. ¹¹ Department of Biological Sciences, Vanderbilt University, Nashville, Tennessee 37235, USA. ¹² Advanced Science Research Center, Kanazawa University, Kanazawa 920-0934, Japan. ¹³ National Institute for Basic Biology (NIBB), Okazaki 444-8585, Japan. ¹⁴ Department of Basic Biology, School of Life Science, Graduate University for Advanced Studies, Okazaki 444-8585, Japan. ¹⁵ Institute of Cytology and Genetics of the Russian Academy of Sciences, Novosibirsk 630090, Russia. * These authors contributed equally to this work. Correspondence and requests for materials should be addressed to T.K. (email: kikawada@affrc.go.jp).

Several organisms have evolved the ability to withstand extreme abiotic stresses, which are lethal for most other forms of life. Anhydrobiosis is a unique ametabolic state that enables a living organism to maintain viability even after losing more than 97% of its body water. Anhydrobiosis is generally associated with extraordinary cross-tolerance to a large variety of extreme conditions, such as temperatures ranging from -270 to $+102$ °C, vacuum and hydrostatic pressures up to 1.2 GPa and extremely high doses of radiation (up to 7,000 Gy)^{1,2}. Anhydrobiotes also exhibit surprising longevity, and certain species have survived tens or even thousands of years in the dry form before recovery on rehydration³.

Among metazoans, the ability to survive severe desiccation by entering an anhydrobiotic state is limited to several groups that include mostly microscopic organisms¹. The largest and most complex anhydrobiotic animal is the larva of a non-biting midge, which is the sleeping chironomid *Polypedilum vanderplanki*^{4,5} (Fig. 1a). Chironomid midges are known for their capacity to adapt to a wide variety of extreme environments and constitute a unique group among insects⁶. However, anhydrobiosis is a complex adaptive trait and *de novo* acquisition of such an extreme desiccation tolerance is most likely a unique evolutionary event. *P. vanderplanki* is the only anhydrobiotic species known to date among both chironomid midges and the entire insect lineage. In contrast to other anhydrobiotes (such as rotifers, tardigrades, nematodes or even plants) that are found in phyla showing widespread desiccation tolerance in a large array of species, *P. vanderplanki* is an isolated case among anhydrobiotes¹. This finding suggests that the sleeping chironomid is a promising model for comparative genomics and should allow a precise dissection of the genetic background underlying the development of tolerance to complete desiccation. Over the last decade, investigations of the sleeping chironomid resulted in the identification of several groups of biomolecules, including late embryogenesis abundant (LEA) proteins, trehalose, antioxidants and heat-shock proteins contributing to desiccation tolerance^{7–13}. In addition, *in vitro* and *in vivo* experiments have shown that these components are necessary but not sufficient to acquire complete desiccation tolerance. Therefore, whole-genome screening for anhydrobiosis-related features became an obligatory

step in further understanding the molecular background of successful desiccation tolerance^{14,15}.

As mentioned above, the adaptation of *P. vanderplanki* is an isolated case of anhydrobiosis among all insects (Fig. 1a). A closely related species from the same genus, *P. nubifer*, is sensitive to desiccation (Fig. 1b). Thus, the combination of *P. vanderplanki* and *P. nubifer* represents a uniquely informative model of comparative genomics for deciphering the entire genetic background of anhydrobiosis.

Our principal aim was to identify genome features specific to *P. vanderplanki* that are lacking in *P. nubifer* and other insects with sequenced genomes (including the fruit fly *Drosophila* and mosquitoes of the genera *Anopheles* and *Aedes*; Fig. 1c). This strategy allowed us to successfully identify several key genomic features accounting for extreme desiccation tolerance in *P. vanderplanki*. Among these features, the most obvious traits characterizing anhydrobiosis are the presence of specific genomic regions containing clusters of multi-copy protective genes involved in desiccation tolerance, the active utilization of protective proteins that most likely originate from horizontal gene transfer (HGT) and new desiccation-driven expression patterns for single genes that already exist in the *P. vanderplanki* genome.

Results

Assembly and characteristics of the chironomid genomes. The ~600-fold coverage sequencing yielded a 104 Mbp for *P. vanderplanki* (scaffold N50 = 229 kbp) and 107 Mbp for *P. nubifer* (scaffold N50 = 26 kbp) genome assemblies (Supplementary Note 1) approximating to the estimated genome sizes (96 and 95 Mb, respectively). A spread of metaphase giant chromosomes revealed a chromosome number of $2n = 8$ for both species (Supplementary Fig. 1). The *P. vanderplanki* genome is characterized by higher AT content and a low number of known transposable elements. The *P. vanderplanki* and *P. nubifer* genomes are predicted to contain 17,137 and 16,553 protein-coding loci, respectively (Supplementary Note 1). The *P. vanderplanki* and *P. nubifer* genome contigs contain 97.18 and 95.56% of the complete core eukaryotic protein-coding sequences, which

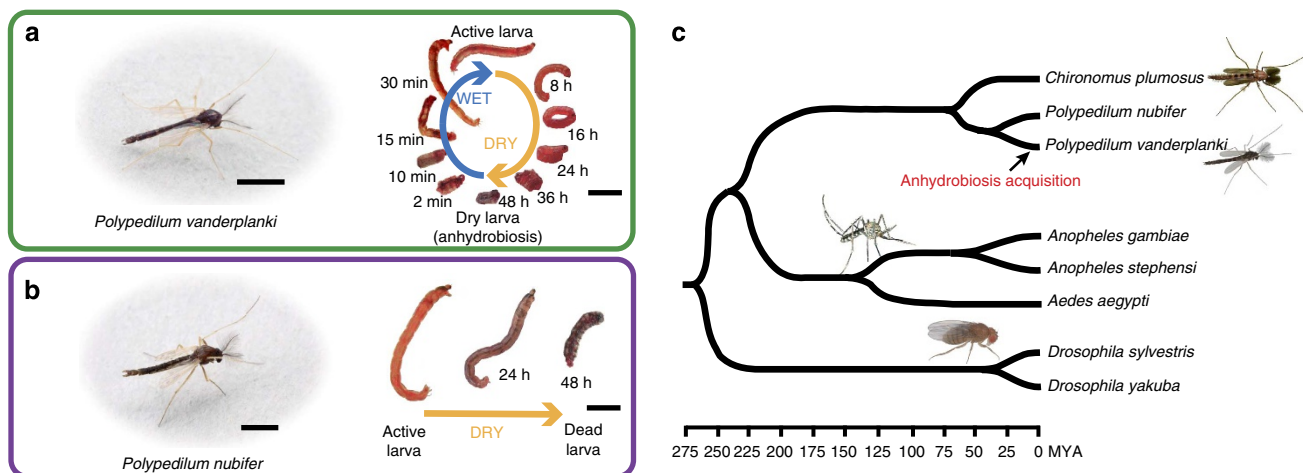


Figure 1 | Desiccation tolerance and phylogeny of two chironomid species. (a) Adult male of the sleeping chironomid, *P. vanderplanki* (left), and anhydrobiotic cycle of the larvae (right). During the dry season, larvae desiccate slowly to reach an ametabolic, quiescent state, termed anhydrobiosis. On rehydration, dried larvae rapidly recover normal activity. (b) Adult male of the congeneric chironomid, *P. nubifer* (left). *P. nubifer* larvae can survive mild desiccation for 24 h like other chironomids, but they cannot enter anhydrobiosis and are killed by severe dehydration (right). Scale bar, 2 mm. (c) Phylogenetic tree inferred from the amino-acid sequence of cytochrome oxidase I (COI) showing the relationship between *P. vanderplanki*, *P. nubifer* and other Diptera. The scale shows the evolutionary distance between species in million years (MYA).

Table 1 | The statistics of the assembled genomes of *P. vanderplanki* and *P. nubifer*.

Species	Number of chromosomes	Size of genome assembly (Mbp)	Scaffold N50 (Mbp)	GC content (%)	Repetitive content (%)	Known transposable element (%)	Predicted number of genes	Number of genes in orthologous clusters with other species	Mean number of exons per gene (with >2 orthologues)	Mean exon length (bp)	Mean intron length (bp)
<i>P. vanderplanki</i>	4	104	0.23	28	5.01	0.26	17,137	14,317	5	324	533
<i>P. nubifer</i>	4	107	0.03	39	3.30	1.26	16,553	13,529	4	328	452

confirms the completeness of genome decoding (Supplementary Note 1). The genome browser ‘MidgeBase’ containing both assembled contigs and mRNA-seq mapping data is accessible at <http://bertone.nises-f.affrc.go.jp/midgebase> (Supplementary Fig. 2). The statistics of the assembled genomes are given in Table 1.

Gene expression in unstressed and desiccated larvae of both species.

The whole-genome transcription profile was different between two chironomid species in desiccation conditions. We estimated the InterProScan domains’ distribution in the proteins predicted to be expressed in the larvae of both species under unstressed conditions. As shown in Supplementary Table 1 and Supplementary Data 1, the primary distribution of domains in *P. vanderplanki* and *P. nubifer* was similar. In contrast, a hypergeometric test (with confidence threshold $P < 1E - 03$) on the annotation of the distribution of the domains upregulated by desiccation for 24 h (D24) in *P. vanderplanki* was exclusively enriched for thioredoxins (TRXs), protein-L-isoaspartate-(D-aspartate) O-methyltransferases (PIMTs), LEA proteins and globins (Supplementary Table 2). Of the 100 *P. vanderplanki* genes showing the highest rate of upregulation during desiccation and abundance in the mRNA pool at different stages of dehydration, the majority are either represented by *P. vanderplanki*-specific loci (having no orthologue in *P. nubifer* or other insects) or was found within the top hits in the desiccation-specific domain-enrichment table (Supplementary Table 2; Supplementary Data 2). Note that in *P. vanderplanki*, the upregulation of gene expression is observed throughout the desiccation process. However, transcriptional activity is most likely to be stopped completely when the dry anhydrobiotic state is reached (D48).

Anhydrobiosis-Related gene Island (ARId). We noticed that in many cases, the genes encoding desiccation-specific mRNAs in *P. vanderplanki* are located in compact clusters in the genome. We defined *P. vanderplanki*-specific genomic regions where these gene sets are located as ‘anhydrobiosis-related gene island’ (ARId) to emphasize a possible contribution to desiccation tolerance. ARIDs share the following common features (Fig. 2): (a) they host a paralogous set of anhydrobiosis-related genes; (b) their localization in the genome is not necessarily related to that of the potential ancestor of the expanded set of genes; and (c) all genes located within ARIDs are upregulated by desiccation¹⁶. Our current data suggest that the *P. vanderplanki* genome contains at least nine potential ARIDs and each contains at least four paralogous highly desiccation-responsive genes (at least threefold increase in expression and RPKM (reads per kilo base of exon model per million mapped reads) value > 10) in the cluster. In contrast, the *P. nubifer* genome contains no regions matching the ARId criteria.

LEA protein genes located in ARIDs. LEA proteins possess chaperone-like or so-called molecular shield activity that protects

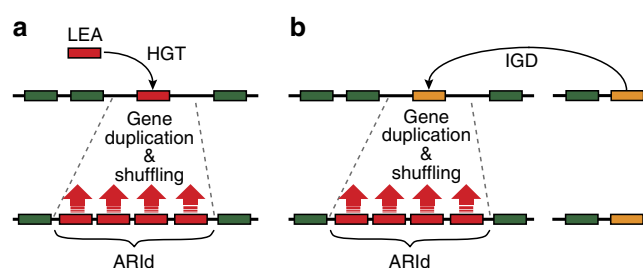


Figure 2 | Putative mechanism for the evolution of ARId in the *P. vanderplanki* genome. ARIDs are genomic regions containing clusters of duplicated genes that are transcriptionally active during anhydrobiosis. (a) A gene of foreign origin (for example, LEA protein) is incorporated into *P. vanderplanki* genome by HGT and undergoes extensive duplications and shuffling. (b) A pre-existing *P. vanderplanki* gene originally not involved in anhydrobiosis and originating from another region of *P. vanderplanki* genome was inserted to a new locus by intragenomic duplication (IGD) and undergoes extensive duplications and shuffling to acquire or improve a specific function for desiccation tolerance. All the genes in the ARIDs from both **a, b** become highly upregulated during anhydrobiosis (red arrows).

proteins and membranes from desiccation stress¹⁷. They have been reported in both plants and invertebrates characterized by tolerance to water depletion¹⁸. Four genes encoding LEA proteins have been reported in *P. vanderplanki*^{9,19}, but not in other insects (including insects with sequenced genomes). Analysis of the *P. vanderplanki* genome revealed 27 LEA protein genes (Supplementary Data 3), but none in the *P. nubifer* genome (Supplementary Data 3). These data suggest that the presence and activity of LEA proteins is correlated with anhydrobiotic capability. While plants have multigene families encoding LEA proteins (for example, 51 genes in *Arabidopsis*²⁰) of which the respective genes are distributed throughout the genome, only a few LEA proteins have been characterized in any particular invertebrate species²¹. At the same time, increasing numbers of transcriptome studies suggest that multiple LEA-like proteins are a feature of at least some anhydrobiotic animals²².

P. vanderplanki genes encoding LEA proteins (*PvLea* genes) are compactly arranged in two ARId clusters in the genome and there are some other genes interspersed¹⁶. None of the interspersed genes have orthologues in other insects or in *P. nubifer*. All predicted LEA-like genes in *P. vanderplanki* were expressed under non-desiccating conditions and most were strongly upregulated by desiccation (Supplementary Data 4)¹⁶. In most cases, desiccated larvae contained the highest level of each *PvLea* mRNA and the mRNA expression returned to control levels in larvae rehydrated for 24 h (Supplementary Data 4).

To obtain insight into the possible origin of LEA protein genes in the *P. vanderplanki* genome, we conducted phylogenetic analyses using the BlastX protocol to identify homologies of *PvLea* genes with other insect genes. However, these analyses did not identify any homologues (Supplementary Data 3). We

expanded the search to other organisms and determined that the *PvLea1* and *PvLea5* genes (the largest length among *Lea* genes in *P. vanderplanki*) had the highest similarity to LEA protein (Ce-LEA-1) from the nematode *Caenorhabditis elegans* and unknown protein (WP_020558683) from a soil bacteria *Thiothrix flexiles*, respectively (Fig. 3, Supplementary Data 3). We found the bacterial protein WP_020558683 significantly corresponded with PvLEA1 and PvLEA5 by comparing LEA proteins in *P. vanderplanki* using BlastP (Supplementary Data 5). The Pfam search showed that both nematode- and bacterial-deduced proteins possessed several repetitions of an 11-mer amino-acid motif, so-called 'LEA_4 motif (PF02987)', which represent a feature of group 3 LEA proteins. On the basis of the studies on the properties of LEA proteins, it is known that their functional activity is defined by the repetitive 11-mer LEA motifs²³. The motif search engine MEME SUITE²⁴ was then employed for further identification of repetitive amino-acid sequences in PvLEA1, PvLEA5 and WP_020558683. The search indicated that the distribution of the motifs in the PvLEA sequences resembled that of *T. flexiles* (a potential prokaryotic donor; Fig. 3). Both chironomid's and the bacterial proteins had similar 11-mer motifs (motif 1 in Fig. 3), which were identical to the typical LEA motif²³. These data imply that *PvLea1* and *PvLea5* were horizontally acquired from soil bacteria in the habitat of *P. vanderplanki*. The gene duplications and shuffling of these ancestral *Lea* genes within the *P. vanderplanki* genome may have generated the large *PvLea* cluster as an ARId (Fig. 2a).

Antioxidants and ARId-specific TRXs. Antioxidants play an important role in the adaptation to extreme dehydration in anhydrobiotes²⁵. The expression of several key antioxidant genes is linked to anhydrobiosis in *P. vanderplanki*. Desiccated larvae accumulate corresponding mRNA and proteins so that during rehydration they can efficiently scavenge reactive oxygen species¹³. We identified 52 genes in *P. vanderplanki* and 29 genes in *P. nubifer* encoding core components of the insect enzymatic antioxidant systems²⁶ (Supplementary Data 6). The number of such genes in *P. nubifer* is similar to that of other insects²⁶. However, in *P. vanderplanki*, several groups of antioxidant genes have expanded (Supplementary Data 6). In addition to the two cytoplasmic and single mitochondrial superoxide dismutases (SOD) that are well conserved among other insects including *P. nubifer*, the *P. vanderplanki* genome possesses two additional genes encoding a Zn-Cu-SOD (Supplementary Data 6). On the basis of sequence similarity and genomic location, these genes are not paralogues of classical insect SOD. These SOD genes are highly expressed in response to desiccation and are most likely involved in anhydrobiosis (Supplementary Data 7). Another remarkable finding is the appearance of additional exons in glutathione peroxidase genes

that result in the formation of splice variants specifically upregulated in the cycle of anhydrobiosis (see Supplementary Note 2 and Supplementary Fig. 3).

TRXs are small redox proteins present in all organisms²⁷. These proteins are involved in redox signalling and act as antioxidants by facilitating the reduction of other proteins via cysteine thiol-disulfide exchange²⁸. The number of TRXs in animal genomes ranges from one to five, and most isoforms are critical for normal organism function²⁹. The two chironomid genomes both contain three TRXs that are well conserved in number and structure among insect genomes (insect TRX-1 to TRX-3 in Fig. 4a). However, the *P. vanderplanki* genome contains 21 additional genes encoding TRXs arranged in two ARIDs unlinked to the classical TRX set of genes (*P. vanderplanki*-specific TRX in Fig. 4a; Supplementary Data 6 and 8). These newly identified TRXs share key features of cytosolic TRX, including small size and a single TRX domain. In addition, all of the genes are strongly upregulated by desiccation. In contrast, the classical TRX genes in *P. vanderplanki* (*PvTrx1–3*) respond only moderately to water loss (Supplementary Data 7).

Unexpected diversity of protein-repair methyltransferases in ARId.

PIMT is an enzyme that recognizes and catalyses the repair of damaged L-isopartyl and D-aspartatyl groups in proteins³⁰. PIMT partially restores aspartic residues in proteins that have been non-enzymatically damaged due to age and extends the life of its substrates. This highly conserved enzyme is present in nearly all eukaryotes, Archaea and gram-negative eubacteria mostly as a single isoform (or as a few isoforms in certain plants and some bacteria)³¹. Insects have a single copy of the PIMT-coding gene like plants, nematodes and mammals. PIMT activity in animals was found to be tightly linked to stress resistance and lifespan^{30,31}. The structure and number of PIMT-coding genes in the two chironomid species varied dramatically. Both species have the orthologues of PIMT shared by dipteran insects (PIMT-1 in Fig. 4b; Supplementary Data 9). *P. nubifer* has only one PIMT gene (*PnPim1*). However, the *P. vanderplanki* genome contains 13 additional genes paralogous to *Pim1* (*PvPim2–14* in Fig. 4b). These genes presumably code for functional PIMT proteins. The genes are arranged in a single cluster¹⁶. Remarkably, the *PvPim1* location in *P. vanderplanki* is not within the single ARId constituting other *Pim*-like genes. The expression of PIMT1-coding gene in both chironomids (*PvPim1* and *PnPim1*) did not change in response to desiccation, but the clustered *PvPim2–14* genes showed upregulation on entering anhydrobiosis (Supplementary Data 9). The abundance of *PvPim2–14* mRNAs was maximal in anhydrobiotic larvae and resembled plant seeds where the accumulation of PIMT provides additional protection for proteins during long periods of dry storage by exerting their repair function on rehydration³². The predicted

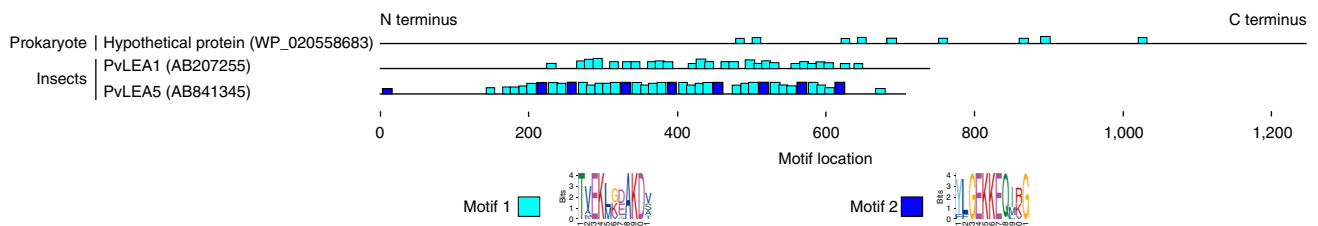


Figure 3 | Amino-acid motif distribution in PvLEA proteins and a bacterial hypothetical protein. The distribution was determined by MEME motif analysis (version 4.9.1). The closest non-eukaryotic genes resembling LEA proteins for *P. vanderplanki* and prokaryotes were identified by a cross-Blast search and used for analysis. The height of the motif block is proportional to $-\log(P \text{ value})$, truncated at the height for a motif with a P value of $1e-10$. MEME parameter settings were as follows: any number of repetitions for the distribution of motif occurrences; 11 for minimum and maximum motif width; and 2 for maximum number of motifs to find.

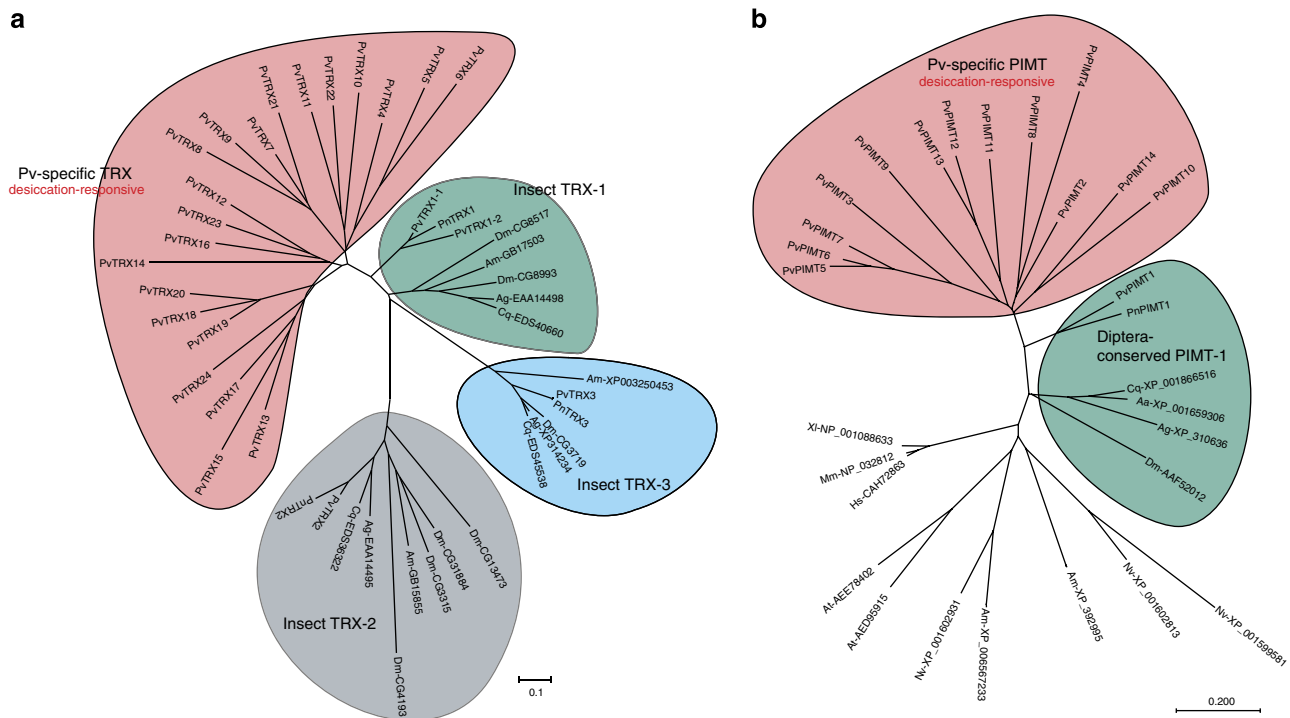


Figure 4 | Evolutionary relationships of the classical and novel desiccation-responsive TRX and PIMT proteins. (a) Phylogenetic tree of TRX proteins showing the clusters of classical insect TRX-1 (green), TRX-2 (grey), TRX-3 (blue) and the cluster of desiccation-responsive TRX, specific to *P. vanderplanki* (pink). (b) Phylogenetic tree of PIMT proteins showing the cluster of the classical PIMT-1 conserved among Diptera (green) and the cluster of desiccation-responsive PIMT proteins, which are specific to *P. vanderplanki* (pink). The evolutionary history was inferred using the neighbor-joining method and the evolutionary distances were computed using the maximum likelihood estimation (units: amino-acid substitutions per site). Pv, *P. vanderplanki*; Pn, *P. nubifer*; Aa, *Aedes aegypti*; Ag, *Anopheles gambiae*; Am, *Apis mellifera*; Cq, *Culex quinquefasciatus*; At, *Arabidopsis thaliana*; Dm, *Drosophila melanogaster*; Hs, *Homo sapiens*; Mm, *Mus musculus*; Nv, *Nasonia vitripennis*; Xi, *Xenopus laevis*.

proteins corresponding to *PvPimt2–14* contain the conserved PIMT functional domain. In addition, the length and structure of the amino- and carboxy-terminal regions of the predicted proteins show marked variation. These findings suggest different substrate preferences or other specific properties of the various *PvPIMTs*. This multi-member family in *P. vanderplanki* is the first observation of large-scale expansion of *Pimt* genes in general and has not been reported in a single insect species.

Haemoglobins and anhydrobiosis. Chironomids are the only group of insects with haemolymph haemoglobins (Hbs) that act as the main respiratory proteins. Thus, chironomid Hbs have a respiratory function analogous to vertebrate Hb. Hbs enhance the O₂ capacity of the haemolymph and enable O₂ transport in the larvae. In addition, Hbs are also assumed to be involved in oxygen storage during periods of hypoxia in poorly aerated water³³. The genomes of the two *Polypedilum* species contain multiple Hb homologues which form several gene clusters. We have identified 33 and 25 *Hb* genes in the *P. vanderplanki* and *P. nubifer* genome, respectively. This study is the first complete genome-based survey of chironomid globins. The structure (represented by both intron-less and intron-bearing orthologues) and multiple nature of the *PvHbs* gene family is similar to that of *P. nubifer* and other midge species³³. However, while the activity of Hb is believed to be mostly larval stage specific, we found that three *PvHb* genes (*PvHb11*, 12 and 21) are exclusively expressed in eggs. This expression is not maternally acquired from adult haemolymph (see MidgeBase browser) as previously suggested³³. Another remarkable difference between the two *Polypedilum* species is that the increased number of *Hb* genes in *P. vanderplanki* results from the insertion of a new cluster of paralogous intron-less *Hb*

genes located in an ARId consisting of six members (see ARId sub-genome browser¹⁶). This gene set (*PvHb11*, 12, 17, 23, 24, 25, 32 and 33 in Supplementary Data 10) is strongly upregulated on desiccation. In contrast, all *PnHb* genes and their orthologous counterparts in *P. vanderplanki* are downregulated in the desiccating larvae (Supplementary Data 10)³³. Four of the 6 anhydrobiotic chironomid-specific *Hb* genes (*PvHb17*, 23, 32 and 33) also showed high mRNA levels under non-stressed conditions and are 4 of the 10 most highly expressed *Hb* genes in the wet larvae (Supplementary Data 10).

Our data on developmental stage-specific and anhydrobiosis process-specific patterns of *Hb* gene expression suggest that the multiple members of this gene family in the chironomids are most likely involved in specialization of the function rather than a general increase in Hb protein dosage, as proposed by some authors³³. One possibility is that the *P. vanderplanki*-specific Hbs may have specific properties allowing them to provide effective delivery of oxygen under conditions of increased molecular crowding in the larvae due to desiccation. Alternatively, the Hbs may protect larvae against free radicals generated during severe dehydration.

Other examples of the process generating ARIDs in *P. vanderplanki* genome (Fig. 2b) are gene clusters coding small heat-shock proteins and several unknown genes¹⁶.

Aquaporins and dehydration process en route to anhydrobiosis. Water channels or aquaporins (AQPs) primarily control permeation of water across the phospholipid bilayer of the cell membrane³⁴. Thus, AQPs most likely play pivotal roles in the dehydration process en route to anhydrobiosis. We have identified five AQP-coding genes in each species of the chironomid (*Aqp1–5*;

Supplementary Table 3), which is a similar number to other dipteran insects^{35,36}. *Aqp1* encodes the water-specific AQP and showed differences in the mRNA-level response to desiccation between the two species. In the anhydrobiotic species, the corresponding gene was strongly responsive to desiccation and its expression increased by more than threefold. The mRNA for *Aqp1* represented more than 80% of all AQP mRNAs in the larvae subjected to slow desiccation. In contrast, expression of *Aqp1* in *P. nubifer* under desiccation did not increase (Supplementary Table 3). *Aqp1* was previously assumed to play a key role in trafficking water out of the body of the anhydrobiotic *P. vanderplanki* larvae³⁷. The current comparative analysis of *P. vanderplanki* and *P. nubifer* *Aqp1* orthologues revealed evolution of specific mRNA regulation in response to desiccation. In *P. vanderplanki*, the total abundance of *Aqp1* mRNA in the larvae was higher under normal conditions and further drastically increased under slow desiccation (Supplementary Table 3).

Anhydrobiosis-related trehalose metabolism pathway. Trehalose is a disaccharide of glucose that stabilizes intact cells in the dry state and replaces water^{1,7,38}. *P. vanderplanki* larvae synthesize large amounts of trehalose (up to 20% dry mass) during dehydration en route to anhydrobiosis^{1,8}. In dehydrated larvae, trehalose stabilizes the structure of biomolecules³⁸. Recently, we isolated genes coding for trehalose-6-phosphate synthase (TPS) and trehalose-6-phosphate phosphatase (TPP). These genes govern trehalose synthesis and trehalase (TREH) hydrolyses trehalose into its component glucose units¹¹. Trehalose is abundantly synthesized from glycogen in the fat body in response to water loss. The elevated sugar concentration is achieved by increased TPS and TPP activities and suppression of TREH activity¹¹. In addition, in *P. vanderplanki*, TRET1 facilitates the transport of trehalose across cellular membranes of the fat body cell¹⁰. TRET1 retains a high capacity for transport activity even when trehalose is highly concentrated in the dehydrating larval body during the final stage of entry into anhydrobiosis¹⁰.

In both chironomids, the genes encoding members of the trehalose metabolism pathway (TMP) including TRET1, TPP, TPS and TREH are represented by single-copy genes (Supplementary Table 4) that are similar to those of other insects both in sequence and gene structure. However, the TMP genes in the two chironomid species responded very differently to desiccation. The expressions of both TPS and TREH were drastically elevated in *P. vanderplanki* but remained unchanged in *P. nubifer*. In contrast, the genes encoding TRET1 and TPP in both species showed a similar pattern of expression and were slightly increased in response to desiccation (Supplementary Table 4). These data suggest that in *P. vanderplanki*, the accumulation of trehalose during the onset of anhydrobiosis is mediated not by a special set of genes (the number and structure of TMP genes in *P. vanderplanki* is similar to that of other insects), but rather by the evolution of gene expression control mechanisms responsive to desiccation.

Another important question is how a simultaneous increase in TREH mRNA and protein¹¹ in the larvae could be associated with a general decrease in the activity of this trehalose-hydrolysing enzyme. Post anhydrobiosis, the rapid decrease in trehalose concentration in the larvae is mediated by TREH activity. Our previous data suggest that the enzyme is stored in the larvae in advance of its requirement during rehydration¹¹.

As mentioned above, TRET1 has a pivotal role for transport of trehalose synthesized in the fat body in the desiccating larvae¹⁰. Other desiccation-inducible transporters might be involved in trehalose uptake in the peripheral tissues on dehydration (see Supplementary Note 3; Supplementary Table 5).

Discussion

Elucidating the origins of ARIDs and the amplification of genes in these regions are critical for understanding the genomics of anhydrobiosis. Desiccation causes extensive DNA damage and anhydrobiotic larvae require several days to repair the damage following rehydration¹³. This DNA damage likely increases the frequency of genome rearrangements. Furthermore, cycles of anhydrobiosis might promote HGT as suggested for rotifers³⁹. A preliminary analysis identified at least 12 expressed genes in the *P. vanderplanki* genome with strong evidence for HGT and these genes are mostly from prokaryotes (Supplementary Table 6). The hypothetical scenario of HGT would be an integration of foreign DNA to the genome of the chironomid from consumed bacteria because it is the primary food source of the larvae. In addition, potential disruptions of cell membranes and severe DNA fragmentation associated with every cycle of anhydrobiosis¹³ are likely to facilitate this process.

The AQP and TMP genes are not located in ARID regions, but show desiccation-responsive expression patterns that are similar to what is observed with the genes from ARID clusters. Examining the *P. vanderplanki* genome and comparing ARIDs and AQP or TMP gene-coding regions are promising models for uncovering the structure of yet unknown desiccation-inducible *cis*-elements and/or *trans*-regulation modules such as transcription factors and noncoding RNAs.

In summary, anhydrobiosis-associated genes (including chaperone-like proteins, antioxidants, aging-related proteins and unique globins) in *P. vanderplanki* have undergone massive expansion within the gene clusters or ARIDs¹⁶. For example, phylogenetic analysis of *PvLea* genes shows that the majority have no significant similarity (BlastP bit score < 100) to LEA protein genes in other organisms and most likely resulted from extensive gene duplication after a founding HGT event (Fig. 2; Supplementary Data 5). Finally, an important event for the evolution of anhydrobiosis in *P. vanderplanki* is the acquisition of new regulatory pathways that are strongly responsive to desiccation. These regulatory pathways control the expression of the gene clusters located in ARID regions and also control isolated genes co-opted for anhydrobiosis (TMP or AQP genes). All these evolutionary changes are likely to be further mediated by *P. vanderplanki* ecology and DNA-damaging effects of desiccation. The nature of *P. vanderplanki* habitats (large isolated rocks), the poor flying ability and strong selection pressure due to the long dry season in semi-arid areas of Africa facilitated microevolutionary patterns in this species. Our recent *in vitro* data show the direct contribution of the members in the expanded gene clusters (such as LEA proteins and antioxidants) to neutralize the effects of desiccation. Another possibility is a non-adaptive gene drift-based origin of the observed changes in *P. vanderplanki* genome. Future comparative investigations on isolated *P. vanderplanki* populations will certainly help to verify these hypotheses for the *de novo* acquisition and the evolution of anhydrobiosis in this unique insect.

Methods

Insects. Highly inbred lines of these sibling species that differ in their ability to resist complete desiccation were used for genomic DNA extraction. *P. vanderplanki* and *P. nubifer* larvae were reared on a 1% agar diet containing 2% commercial milk under controlled photoperiod (13 h light: 11 h dark) and temperature (27–28 °C) conditions.

Number of chromosomes of *P. vanderplanki* and *P. nubifer*. We observed polytene chromosomes in the salivary glands of fully hydrated larvae of *P. vanderplanki* and *P. nubifer*. Fourth instar larvae were fixed in a 3:1 mixture of 96% ethanol and glacial acetic acid and stored at –80 °C until use. Salivary glands were dissected out and stained in 1.0% orcein in 45% acetic acid. They were then washed lightly in 45% acetic acid and squashed in 50% lactic acid.

Estimation of the chironomids' genome sizes by flow cytometry. The genome sizes of the two species were determined by flow cytometry (Cornette *et al.*, in prep). Briefly, heads of adult chironomids were homogenized into a solution of 0.5% Triton X-100 in 1 ml phosphate buffered saline buffer, before staining the nuclei with $5 \mu\text{g ml}^{-1}$ of propidium iodide and filtering on a 30- μm mesh filter (Partec, Münster, Germany). The DNA content of stained nuclei was measured by a Coulter Epics Elite flow cytometry system (Beckman Coulter, Indianapolis, IN). The 2C DNA content of the sample was compared with the standard 0.36 pg DNA of *D. melanogaster* diploid nuclei.

Genomic DNA sampling. Genomic DNA from over 500 final instar larvae (of ~ 1 mg wet body weight) for construction of mate-pair libraries and other experiments was isolated with conventional cetrimonium bromide (CTAB) method⁴⁰ and NucleoSpin tissue (Macheley-Nagel, Düren, Germany), respectively.

Genome sequencing. Genome sequences were obtained using paired-end and mate-pair protocols on Illumina HiSeq 2000, GAIIX and SOLiD 4 instruments. Genomic DNA was fragmented, libraries prepared and sequencing conducted according to the manufacturer's protocols. Mate-paired libraries for the SOLiD 4 system (Life Technologies, Carlsbad, CA) with inserts of ~ 2.5 kb were constructed from 5 μg of genomic DNA, and deposited on two quarters of a flow cell for each sample. Fifty base reads were obtained from each of the F3 and R3 tags, with 22 Gbp for both *P. vanderplanki* and *P. nubifer* libraries. To construct the libraries for whole-genome sequencing, DNA was processed using a TruSeq DNA Sample Preparation kit v.2 (Illumina, San Diego, CA) according to the manufacturer's instructions. Library lengths, as assessed using an Agilent 2100 Bioanalyzer (Agilent Technologies, Santa Clara, CA), were 541 for *P. nubifer* and 397 for *P. vanderplanki*. Libraries were quantified using fluorometry with Qubit 2.0 (Life Technologies) and real-time PCR, and diluted to final concentration of 9 pM. Diluted libraries were clustered using a cBot instrument (Illumina) with a TruSeq PE Cluster Kit v3 (Illumina) and sequenced using a HiSeq 2000 sequencer (Illumina) with TruSeq SBS Kit v3-HS (Illumina), read length 101 from each end. Poly A-mRNA libraries were constructed using TruSeq RNA Sample Preparation kit v.2 (Illumina) and quantified and sequenced in the same way as genomic DNA libraries. For the *P. vanderplanki* genome, sequencing with a single-molecule real-time sequencer was also performed. Approximately 6- and 10-kb insert libraries were constructed and sequenced with C2 chemistry using PacBio RS (Pacific Bioscience, Menlo Park, CA) for 34 cells (version 2).

Using two types of libraries, the GAIIX platform generated a total of 36.8 Gbp of *P. vanderplanki* sequence data (Supplementary Table 7). Furthermore, the HiSeq 2000 platform produced 6.9 Gbp of sequence data, the SOLiD 4 system generated 20.9 Gbp data and the PacBio RS yielded 1,479,033 reads with 1.7–2.7 kb mean maximum subread length, total 2.9 Gbp of independent fragment reads. On the basis of the genome size estimation of 100 Mbp (see above), the total of 67.5 Gbp of sequence data obtained corresponds to ~ 562 -fold coverage of the *P. vanderplanki* genome (Supplementary Table 7). In the case of *P. nubifer*, the HiSeq 2000 platform generated 7.0 Gbp sequence data, providing ~ 58 -fold coverage of that chironomid genome (Supplementary Table 8).

Genome sequence assembly. The shotgun, paired-end and mate-pair reads were assembled *de novo* by the Platanus Assembler⁴¹ (<http://platanus.bio.titech.ac.jp>) and the remaining gaps were filled with PacBio RS reads using the PBJelly pipeline⁴².

Fosmid-end sequences. The fosmid library of *P. vanderplanki* genome was prepared by Takara Bio (Shiga, Japan). Randomly selected fosmid clones were end sequenced by the Sanger method using an ABI 3130xl sequencer (Life Technologies).

Evaluation of assembly with core eukaryotic genes. Gene coverage of the *P. vanderplanki* and *P. nubifer* genome assemblies was evaluated with 248 core eukaryotic genes using CEGMA 2.4 (Core Eukaryotic Genes Mapping Approach)⁴³.

Repetitive and transposon-like regions in the genomes. We ran RepeatModeler⁴⁴ with default parameters to identify *de novo* repeat elements and classify them automatically. The programme internally incorporates three *de novo* repeat finders, that is, RECON⁴⁵, RepeatScout⁴⁶ and TRF (Tandem Repeat Finder)⁴⁷ and generates libraries of repeat sequences.

Transcriptome sequencing and mapping. Transcriptome analysis is essential to understand gene expression profiles in specific organisms. For more effective prediction of the gene models and genetic network associated with desiccation resistance, we performed complex mRNA expression analysis of the two chironomids, combining known expressed sequence tag (EST) databases⁴⁸ and newly prepared data with the aid of next-generation sequencing technologies.

We obtained 454 ESTs from the *P. vanderplanki* complementary DNA (cDNA) library using the 454 GS FLX Titanium platform (454 Life Science, Branford, CT). The cDNA library for 454 ESTs was prepared according to Meyer *et al.*⁴⁹ and sequenced according to manufacturer's instructions. A total of 885,642 reads, with an average length of 355 bp, resulted in over 314 Mbp of data. Before downstream analysis, adaptor and vector sequences in the raw tags were trimmed with SeqClean⁵⁰ software and UniVec database⁵¹. This pre-process resulted in 852,333 high-quality reads with a minimum length of 100 bp.

High-throughput mRNA sequencing (RNA-seq) offers the ability to discover new genes and transcripts and measure transcript expression in a single assay. To develop comprehensive insight into differential gene expression during dehydration and rehydration and to improve coverage of transcriptome data, we performed deep RNA sequencing from various RNA samples. Total RNA from four hydrated, dehydrating and rehydrated (*P. vanderplanki* only) larvae (each of 50 individuals) was extracted using Trizol (Life Technologies) and the RNeasy Mini Kit (Qiagen, Hilden, Germany), according to the manufacturer's recommendations. TruSeq RNA Sample Preparation kit v.2 (Illumina) was used for preparation of RNA-seq libraries. For *P. vanderplanki*, RNA was collected from whole larvae at 0, 24 and 48 h of dehydration (each of 50 individuals). RNA was also sampled from whole larvae at 3 and 24 h after rehydration. For *P. nubifer*, RNA was sampled from whole larvae only at 0 and 24 h of dehydration (each of 50 individuals). These samples were subjected to deep sequencing on the Illumina GA II platform. In the same manner, RNA from four life stages (eggs, larvae, pupae and adults) for *P. vanderplanki* and one stage (larvae) for *P. nubifer* was extracted and sequenced on the Illumina HiSeq 2000 platform. RNA-seq reads' source data are summarized in Supplementary Table 9.

Gene prediction. Gene model predictions were generated using AUGUSTUS software (version 2.6.1)^{52,53}. Because of the unavailability of species parameters for *P. vanderplanki* and *P. nubifer*, we first trained AUGUSTUS to create the parameter sets for both species. We adopted iterated training using predicted genes generated with the existing parameter set for *Anopheles gambiae*. After iterated training, parameters were adjusted with the built-in Perl script, `optimize_augustus.pl`, to optimize prediction accuracy. We also constructed extrinsic evidence about genes from available transcriptome data, including Sanger ESTs, 454 ESTs and RNA-seq reads. Sanger ESTs were mapped onto genomic sequences using GMAP⁵⁴. ESTs from the 454 FLX platform were assembled into contigs using MIRA3 (ref. 55) before the mapping process and were aligned to the genome with BLAT⁵⁶. RNA-seq reads were assembled into transcripts using TopHat2 (ref. 57) and Cufflinks⁵⁸. Protein genome alignment data between *A. gambiae* and *Aedes aegypti* protein and genomic sequences, generated with Exonerate⁵⁹, were also incorporated. The complete data set was merged into a 'hint file' and used for gene prediction. The resultant numbers of genes for *P. vanderplanki* and *P. nubifer* were 17,824 and 17,224, respectively. All RNA-seq reads (Supplementary Table 9) were mapped onto gene models using Bowtie2 (ref. 60) with default parameters to estimate expression level (RPKM). We filtered out all genes with either an RPKM value of 0 or a raw tag count below 2 in all samples. This process discarded 207 and 394 genes of *P. vanderplanki* and *P. nubifer*, respectively. Transposable element-derived proteins were also filtered out based on automated annotation results, including InterProScan and BlastP (1e–05, no filter). The final *P. vanderplanki* gene model set contained 17,137 genes and the final gene model set for *P. nubifer* consisted of 16,553 genes (Supplementary Table 10).

Identification of chironomid genes. Predicted genes were annotated using a set of publicly available tools. We performed BlastP (version 2.2.25)⁶¹ searches of gene models against NCBI-nr with an expectation value of $1.0e-05$. As a result, for *P. vanderplanki* and *P. nubifer*, 2,558 out of 14,579 (17.5%) and 3,201 out of 13,352 (24.0%) genes did not have a significant hit, respectively. Protein domain annotation of gene models was done by combination of HMMER3 and domain models' Pfam A^{62,63}. To obtain more comprehensive information on protein function, all deduced proteins were subjected to InterProScan (version 4.8) analysis. The result of annotation for all *P. vanderplanki* and *P. nubifer* genes, together with the expression data (RPKM), was prepared as a single MS-Excel file (Supplementary Data 11). The frequency of Gene Ontology terms and InterPro IDs⁶⁴ for *P. vanderplanki* and *P. nubifer* were also summarized (Supplementary Data 1).

Estimation of expression of the predicted genes. The mRNA expression levels for the entire transcript set (Supplementary Table 9) were estimated using the RPKM values. For confident comparison of the transcriptional response to desiccation in the two chironomids, only two sets of data (wet larvae versus larvae desiccated for 24 h, termed D0 and D24) were used. An increase in expression of more than threefold and an RPKM value > 10 for the higher value were used as the criteria for placement of a gene in the 'desiccation-responsive' group. The expression data were represented by tracks in the genome browser.

Genome browser. A genome browser for the assembled genome sequences has been established using the Generic Genome Browser (GBrowse) 2.17 (ref. 65)

(Supplementary Fig. 2), incorporating both the genome structure of the two chironomid species and genome-wide mRNA expression data in response to desiccation (*P. nubifer*) and for the complete cycle of anhydrobiosis (*P. vanderplanki*). The URL for the browser is: Midgebase <http://bertone.nises-f.affrc.go.jp/midgebase>; GBrowse for *P. vanderplanki* <http://bertone.nises-f.affrc.go.jp/cgi-bin/gb2/gbrowse/pv091>; GBrowse for *P. nubifer* <http://bertone.nises-f.affrc.go.jp/cgi-bin/gb2/gbrowse/pn090>; and GBrowse for ARIDs <http://bertone.nises-f.affrc.go.jp/cgi-bin/gb2/gbrowse/arid/>.

Alignment of the sequences and building the phylogenetic trees. A phylogenetic tree of *P. vanderplanki* in dipteran species inferred from the amino-acid sequence of cytochrome oxidase I (COI) was adapted from several previous analyses^{66–69}. The deduced protein sequences were used to reconstruct phylogeny of TRX and PIMT in *P. vanderplanki* and *P. nubifer*. The alignment was done using MUSCLE⁷⁰ in CLC Main Workbench 6 (CLC bio, Aarhus, Denmark) and the trees were built using neighbour joining with 1,000 bootstraps. The reference orthologous genes from other insects were derived from the public database.

Pipeline for identification of horizontally transferred genes. We used a custom phylogenomic pipeline to build gene trees for all predicted coding regions in *P. vanderplanki* and *P. nubifer*; scripts are available from the authors on request. Predicted amino-acid sequences were first queried using BlastP against a local database consisting of NCBI's Reference Sequence and predicted protein sequences from recently sequenced microbial eukaryotes (JGI genome portal and Ghent University's online genome annotation server BOGAS). For each Blast result, a hit was considered significant if the *E*-value was $\leq 1e-3$, the bit score was ≥ 60 and fraction conserved was ≥ 0.3 . If a hit met these sequence similarity thresholds, the associated sequence was extracted from the database using a custom Perl script. To reduce the number of paralogues in the analysis, only the top four hits per species were extracted. Extracted sequences were reordered based on global similarity to the query sequence with MAFFT using the minimum linkage clustering method and rough distance measurement (number of shared 6-mers)⁷¹. After reordering, the files were reduced to include only the top 200 sequences, and files with fewer than 4 sequences were eliminated. Alignments were performed with MAFFT using the automated strategy selection. Poorly aligned positions and sequences were removed from the alignment using REAP⁷², and trimmed alignments were further refined by a second MAFFT alignment using the same parameters as above. Phylogenetic trees were inferred using FastTree, assuming a JTT + CAT amino-acid model of substitution and 1,000 bootstrap replicates⁷³. For each tree, the phylogenetic sister group to *Polypedium* was determined using SICLE⁷⁴ (<http://eebweb.arizona.edu/sicle/>). Finally, the candidate genes were analysed manually to filter out potential false-positive cases. The results of final screening are summarized in Supplementary Table 6.

References

- Watanabe, M. Anhydrobiosis in invertebrates. *Appl. Entomol. Zool.* **41**, 15–31 (2006).
- Horikawa, D. D. *et al.* High hydrostatic pressure tolerance of four different anhydrobiotic animal species. *Zool. Sci.* **26**, 238–242 (2009).
- Sallon, S. *et al.* Germination, genetics, and growth of an ancient date seed. *Science* **320**, 1464 (2008).
- Wharton, D. A. *Life at the Limits: Organisms in Extreme Environments* 307 (Cambridge Univ. Press, 2002).
- Hinton, H. E. A fly larva that tolerates dehydration and temperatures of -270° to $+102^{\circ}$ C. *Nature* **188**, 336–337 (1960).
- Cranston, P. S. in: *The Chironomidae: Biology and Ecology of Non-Biting Midges*. (eds Armitage, P., Cranston, P. S. & Pinder, L. C. V.) Ch. 1, 1–7 (Chapman & Hall, 1995).
- Cornette, R. & Kikawada, T. The induction of anhydrobiosis in the sleeping chironomid: current status of our knowledge. *IUBMB Life* **63**, 419–429 (2011).
- Watanabe, M., Kikawada, T., Minagawa, N., Yukuhiro, F. & Okuda, T. Mechanism allowing an insect to survive complete dehydration and extreme temperatures. *J. Exp. Biol.* **205**, 2799–2802 (2002).
- Kikawada, T. *et al.* Dehydration-induced expression of LEA proteins in an anhydrobiotic chironomid. *Biochem. Biophys. Res. Commun.* **348**, 56–61 (2006).
- Kikawada, T. *et al.* Trehalose transporter 1, a facilitated and high-capacity trehalose transporter, allows exogenous trehalose uptake into cells. *Proc. Natl Acad. Sci. USA* **104**, 11585–11590 (2007).
- Mitsumasu, K. *et al.* Enzymatic control of anhydrobiosis-related accumulation of trehalose in the sleeping chironomid *Polypedium vanderplanki*. *FEBS J.* **277**, 4215–4228 (2010).
- Gusev, O., Cornette, R., Kikawada, T. & Okuda, T. Expression of heat shock protein-coding genes associated with anhydrobiosis in an African chironomid *Polypedium vanderplanki*. *Cell Stress Chaperones* **16**, 81–90 (2011).
- Gusev, O. *et al.* Anhydrobiosis-associated nuclear DNA damage and repair in the sleeping chironomid: linkage with radioresistance. *PLoS ONE* **5**, e14008 (2010).
- Li, S. *et al.* Late embryogenesis abundant proteins protect human hepatoma cells during acute desiccation. *Proc. Natl Acad. Sci. USA* **109**, 20859–20864 (2012).
- Marunde, M. R. *et al.* Improved tolerance to salt and water stress in *Drosophila melanogaster* cells conferred by late embryogenesis abundant protein. *J. Insect Physiol.* **59**, 377–386 (2013).
- Suetsugu, Y., Gusev, O., Cornette, R. & Kikawada, T. ARID sub-genome browser <<http://bertone.nises-f.affrc.go.jp/cgi-bin/gb2/gbrowse/arid/>> (2013).
- Tunnaciff, A., Hincha, D., Leprince, O. & Macherel, D. in: *Topics in Current Genetics* Vol. 56 (eds Lubzens, E., Cerda, J. & Clark, M.) 91–108 (Springer, 2010).
- Hand, S. C., Menze, M. A., Toner, M., Boswell, L. & Moore, D. LEA proteins during water stress: not just for plants anymore. *Annu. Rev. Physiol.* **73**, 115–134 (2011).
- Hatanaka, R. *et al.* An abundant LEA protein in the anhydrobiotic midge, PvLEA4, acts as a molecular shield by limiting growth of aggregating protein particles. *Insect Biochem. Mol. Biol.* **43**, 1055–1067 (2013).
- Bies-Etheve, N. *et al.* Inventory, evolution and expression profiling diversity of the LEA (late embryogenesis abundant) protein gene family in *Arabidopsis thaliana*. *Plant Mol. Biol.* **67**, 107–124 (2008).
- Pouchkina-Stantcheva, N. N. *et al.* Functional divergence of former alleles in an ancient asexual invertebrate. *Science* **318**, 268–271 (2007).
- Forster, F. *et al.* Transcriptome analysis in tardigrade species reveals specific molecular pathways for stress adaptations. *Bioinform. Biol. Insights* **6**, 69–96 (2012).
- Shimizu, T. *et al.* Desiccation-induced structuralization and glass formation of group 3 late embryogenesis abundant protein model peptides. *Biochemistry* **49**, 1093–1104 (2010).
- Bailey, T. L. *et al.* MEME SUITE: tools for motif discovery and searching. *Nucleic Acids Res.* **37**, W202–W208 (2009).
- Kranner, I. & Birtic, S. A modulating role for antioxidants in desiccation tolerance. *Integr. Comp. Biol.* **45**, 734–740 (2005).
- Corona, M. & Robinson, G. E. Genes of the antioxidant system of the honey bee: annotation and phylogeny. *Insect Mol. Biol.* **15**, 687–701 (2006).
- Meyer, Y. *et al.* Glutaredoxins and thioredoxins in plants. *Biochim. Biophys. Acta* **1783**, 589–600 (2008).
- Forster, F. *et al.* Tardigrade workbench: comparing stress-related proteins, sequence-similar and functional protein clusters as well as RNA elements in tardigrades. *BMC Genomics* **10**, 469 (2009).
- Wu, Z. & Xing, J. Functional roles of slow enzyme conformational changes in network dynamics. *Biophys. J.* **103**, 1052–1059 (2012).
- Khare, S., Linster, C. & Clarke, S. The interplay between protein L-isoaspartyl methyltransferase activity and insulin-like signaling to extend lifespan in *Caenorhabditis elegans*. *PLoS ONE* **6**, e20850 (2011).
- Desrosiers, R. R. & Fanelus, I. Damaged proteins bearing L-isoaspartyl residues and aging: a dynamic equilibrium between generation of isomerized forms and repair by PIMT. *Curr. Aging Sci.* **4**, 8–18 (2011).
- Lowenson, J. D. & Clarke, S. Structural elements affecting the recognition of L-isoaspartyl residues by the L-isoaspartyl/D-aspartyl protein methyltransferase. Implications for the repair hypothesis. *J. Biol. Chem.* **266**, 19396–19406 (1991).
- Burmester, T. & Hankeln, T. The respiratory proteins of insects. *J. Insect Physiol.* **53**, 285–294 (2007).
- Agre, P. & Kozono, D. Aquaporin water channels: molecular mechanisms for human diseases. *FEBS Lett.* **555**, 72–78 (2003).
- Drake, L. L. *et al.* The Aquaporin gene family of the yellow fever mosquito, *Aedes aegypti*. *PLoS ONE* **5**, e15578 (2010).
- Spring, J. H., Robichaux, S. R. & Hamlin, J. A. The role of aquaporins in excretion in insects. *J. Exp. Biol.* **212**, 358–362 (2009).
- Kikawada, T. *et al.* Dehydration-inducible changes in expression of two aquaporins in the sleeping chironomid, *Polypedium vanderplanki*. *Biochim. Biophys. Acta* **1778**, 514–520 (2008).
- Sakurai, M. *et al.* Vitricification is essential for anhydrobiosis in an African chironomid, *Polypedium vanderplanki*. *Proc. Natl Acad. Sci. USA* **105**, 5093–5098 (2008).
- Gladyshev, E. A., Meselson, M. & Arkipova, I. R. Massive horizontal gene transfer in bdelloid rotifers. *Science* **320**, 1210–1213 (2008).
- Sambrook, J. & Russell, D. W. *Molecular Cloning: A Laboratory Manual* 3rd edn (Cold Spring Harbor Laboratory Press, 2001).
- Kajitani, R. *et al.* Efficient *de novo* assembly of highly heterozygous genomes from whole-genome shotgun short reads. *Genome Res.* **24**, 1384–1395 (2014).
- English, A. C. *et al.* Mind the gap: upgrading genomes with Pacific Biosciences RS long-read sequencing technology. *PLoS ONE* **7**, e47768 (2012).
- Parra, G., Bradnam, K. & Korf, I. CEGMA: a pipeline to accurately annotate core genes in eukaryotic genomes. *Bioinformatics* **23**, 1061–1067 (2007).
- Smit, A. F. A. & Hubley, R. RepeatMasker Open-1.0 <<http://www.repeatmasker.org>> (2008–2010).
- Bao, Z. & Eddy, S. R. Automated *de novo* identification of repeat sequence families in sequenced genomes. *Genome Res.* **12**, 1269–1276 (2002).

46. Price, A. L., Jones, N. C. & Pevzner, P. A. De novo identification of repeat families in large genomes. *Bioinformatics* **21**(Suppl 1): i351–i358 (2005).
47. Benson, G. Tandem repeats finder: a program to analyze DNA sequences. *Nucleic Acids Res.* **27**, 573–580 (1999).
48. Cornette, R. *et al.* Identification of anhydrobiosis-related genes from an expressed sequence tag database in the cryptobiotic midge *Polypedilum vanderplanki* (Diptera: Chironomidae). *J. Biol. Chem.* **285**, 35889–35899 (2010).
49. Meyer, E. *et al.* Sequencing and de novo analysis of a coral larval transcriptome using 454 GSFlx. *BMC Genomics* **10**, 219 (2009).
50. Pertea, G. SeqClean <<http://compbio.dfci.harvard.edu/tgi/software/>> (2005–2006).
51. NCBI. The UniVec Database <<http://www.ncbi.nlm.nih.gov/tools/vecscreen/univec/>> (2013).
52. Stanke, M., Schoffmann, O., Morgenstern, B. & Waack, S. Gene prediction in eukaryotes with a generalized hidden Markov model that uses hints from external sources. *BMC Bioinformatics* **7**, 62 (2006).
53. Stanke, M., Steinkamp, R., Waack, S. & Morgenstern, B. AUGUSTUS: a web server for gene finding in eukaryotes. *Nucleic Acids Res.* **32**, W309–W312 (2004).
54. Wu, T. D. & Watanabe, C. K. GMAP: a genomic mapping and alignment program for mRNA and EST sequences. *Bioinformatics* **21**, 1859–1875 (2005).
55. Chevreaux, B., Wetter, T. & Suhai, S. Genome sequence assembly using trace signals and additional sequence information. *Proceedings of the German Conference on Bioinformatics (GCB)* **99**, 45–56 (1999).
56. Kent, W. J. BLAT—the BLAST-like alignment tool. *Genome Res.* **12**, 656–664 (2002).
57. Kim, D. *et al.* TopHat2: accurate alignment of transcriptomes in the presence of insertions, deletions and gene fusions. *Genome biology* **14**, R36 (2013).
58. Trapnell, C. *et al.* Transcript assembly and quantification by RNA-Seq reveals unannotated transcripts and isoform switching during cell differentiation. *Nat. Biotechnol.* **28**, 511–515 (2010).
59. Slater, G. S. & Birney, E. Automated generation of heuristics for biological sequence comparison. *BMC Bioinformatics* **6**, 31 (2005).
60. Langmead, B. & Salzberg, S. L. Fast gapped-read alignment with Bowtie 2. *Nat. Methods* **9**, 357–359 (2012).
61. Altschul, S. F., Gish, W., Miller, W., Myers, E. W. & Lipman, D. J. Basic local alignment search tool. *J. Mol. Biol.* **215**, 403–410 (1990).
62. Bateman, A. *et al.* The Pfam protein families database. *Nucleic Acids Res.* **30**, 276–280 (2002).
63. Finn, R. D. *et al.* The Pfam protein families database. *Nucleic Acids Res.* **36**, D281–D288 (2008).
64. Zdobnov, E. M. & Apweiler, R. InterProScan—an integration platform for the signature-recognition methods in InterPro. *Bioinformatics* **17**, 847–848 (2001).
65. Stein, L. D. *et al.* The generic genome browser: a building block for a model organism system database. *Genome Res.* **12**, 1599–1610 (2002).
66. Demin, A. G., Polukonova, N. V. & Muge, N. S. Molecular phylogeny and the time of divergence of mites (Chironomidae, Nematocera, Diptera) inferred from a partial nucleotide sequence of the cytochrome oxidase I gene (*COI*). *Russ. J. Genet.* **47**, 1168–1180 (2011).
67. Dixit, J. *et al.* Phylogenetic inference of Indian malaria vectors from multilocus DNA sequences. *Infect. Genet. Evol.* **10**, 755–763 (2010).
68. Papoucheva, E., Proviz, V., Lambkin, C., Goddeeris, B. & Blinov, A. Phylogeny of the endemic Baikalian *Sergentia* (Chironomidae, Diptera). *Mol. Phylogenet. Evol.* **29**, 120–125 (2003).
69. Grimaldi, D. & Engel, M. S. *Evolution of the Insects* 755 (Cambridge Univ. Press, 2005).
70. Edgar, R. C. MUSCLE: multiple sequence alignment with high accuracy and high throughput. *Nucleic Acids Res.* **32**, 1792–1797 (2004).
71. Katoh, K. & Standley, D. M. MAFFT multiple sequence alignment software version 7: improvements in performance and usability. *Mol. Biol. Evol.* **30**, 772–780 (2013).
72. Hartmann, S. & Vision, T. Using ESTs for phylogenomics: can one accurately infer a phylogenetic tree from a gappy alignment? *BMC Evol. Biol.* **8**, 95 (2008).
73. Price, M. N., Dehal, P. S. & Arkin, A. P. FastTree: computing large minimum evolution trees with profiles instead of a distance matrix. *Mol. Biol. Evol.* **26**, 1641–1650 (2009).
74. DeBlasio, D. & Wiscaver, J. SICLE: a high-throughput tool for extracting evolutionary relationships from phylogenetic trees. Preprint at <http://arXiv:1303.5785> [q-bio.GN] (2013).

Acknowledgements

We extend our gratitude to the Federal Ministry of Environment of Nigeria for permitting research on *P. vanderplanki*. We acknowledge Y. Saito and T. Shiratori for their help with rearing and maintenance of midges and larvae, and Y. Sato for preparing sequencing libraries and for other technical assistance with sequencing. A part of sequencing was supported by OIST internal fund to the Marine Genomics Unit, NIAS internal fund and NIBB internal fund. The supercomputing was supported by the IT Section of OIST and NIAS. A part of computation was performed on the Supercomputer System in National Institute of Genetics. This work was supported in part by Grants-in-Aids from MEXT/JSPS KAKENHI (Grant Number 21688004, 22128001, 23128512, 23780055, 24120006, 25128714 and 25252060), Japan; subsidy of the Russian Government to support the Program of competitive growth of Kazan Federal University among world class academic centres and universities; Russian Foundation for Basic Research (No 12-08-33157 mol_a_ved and No 14-04-01657_A); grant 11.G34.31.0008 from the Ministry of Education and Science of the Russian Federation; RFBR and Tatarstan government grant No 12-04-9707.

Authors contributions

T.Ki., N.S., O.G., R.C., A.S.K., T.O., and Y.S. designed and coordinated the project. M.D.L., Y.S., A.A.P., R.K., T.N., D.A., Va.G., Y.K., H.K., Sa.S., T.M., Ve.G., T.Ka., M.F., Sh.S., T.F.S. and M.H. performed genome and EST sequencing and assembly, and chromosome analysis; O.G., Y.S., R.C., T.Ka., R.H., S.K., E.S., T.N., Sh.S., A.M., J.W., M.H. and T.Ki. conducted annotation and analysis. O.G., T.Ka., N.S., T.N., R.C., Y.S. and T.Ki. prepared the manuscript.

Additional information

Accession codes: Sequence data for *P. vanderplanki* and *P. nubifer* have been deposited in GenBank/EMBL/DDJB nucleotide core database under the accession codes PRJDB1558 and PRJDB2914, respectively.

Supplementary Information accompanies this paper at <http://www.nature.com/naturecommunications>

Competing financial interests: The authors declare no competing financial interests.

Reprints and permission information is available online at <http://npg.nature.com/reprintsandpermissions/>

How to cite this article: Gusev, O. *et al.* Comparative genome sequencing reveals genomic signature of extreme desiccation tolerance in the anhydrobiotic midge. *Nat. Commun.* **5**:4784 doi: 10.1038/ncomms5784 (2014).



This work is licensed under a Creative Commons Attribution-NonCommercial-ShareAlike 4.0 International License. The images or other third party material in this article are included in the article's Creative Commons license, unless indicated otherwise in the credit line; if the material is not included under the Creative Commons license, users will need to obtain permission from the license holder to reproduce the material. To view a copy of this license, visit <http://creativecommons.org/licenses/by-nc-sa/4.0/>